Optimal generation scheduling of interconnected wind-coal intensive power systems

Optimal Generation Scheduling of Interconnected Wind-Coal Intensive Power Systems

Songyan Wang[1, 2], Daren Yu[1], Jilai Yu[2], Wei Zhang[2], Aoife Foley[3], Kang Li[4],

1. *Postdoctoral Research Station of Power Engineering and Engineering Thermalphysics, Harbin Institute of Technology, Harbin, China*
2. *School of Electrical Engineering and Automation, Harbin Institute of Technology, Harbin, China*
3. *School of Mechanical and Aerospace Engineering, Queen's University Belfast, United Kingdom*
4. *School of Electronics, Electrical Engineering and Computer Science, Queen's University Belfast, United Kingdom*

* *Corresponding author. Tel.: +44-(0)7462729260; fax: +44-(0)2890975449.*

E-mail address: wangsongyan@163.com (Songyan Wang)

Abstract

Large scale wind power generation complicated with restrictions on the tie line plans may lead to significant wind power curtailment and deep cycling of coal units during the valley load periods. This paper proposes a dispatch strategy for interconnected wind-coal intensive power systems. Wind power curtailment and cycling of coal units are included in the economic dispatch analysis of regional systems. Based on the day-ahead dispatch results, a tie line power plan adjustment strategy is implemented in the event of wind power curtailment or deep cycling occurring in the economic dispatch model, with the objective of reducing such effects. The dispatch strategy is designed based on the distinctive operation characteristics of interconnected wind-coal intensive power systems, and dispatch results for regional systems in China show that the proposed strategy is feasible and can improve the overall system operation performance.

Key word: wind power, interconnections, generation scheduling, coal cycling, wind-coal intensive system

Nomenclature

Acronyms

SE sending end system

RE receiving end system

ASE power adjustment model of the SE

ARE power adjustment model of the RE

EPAC excessive power accommodation capability

UC unit commitment

WCIS wind-coal intensive power system

IWCIS interconnected system with WCIS and load center

Sets

Ω_{br} set of branch lines in RE

Ω_{bs} set of branch lines in SE

Ω_{dps} set of deep cycling units in SE

Ω_{gr} Set of normal units in RE

Ω_{gs} Set of normal units in the SE

Ω_{ws} Set of wind farms in the SE

SE modelling

Objective functions

C_{com} total operation cost in SE

C_{cur} cost of the wind power curtailment in SE

C_{dcyc} deep cycling cost of the deep cycling units in SE

C_{dnom} normal status cost of the deep cycling units in SE

C_{gnom} operation cost of normal units in SE

C_{res} spinning reserve cost in SE

C_{tot} total operation cost of deep cycling unit

$f_{\text{dnom},j}$ normal status cost function of the deep cycling unit j

$f_{\text{gnom},i}$ operation cost function of the normal unit i

Parameters

D_{dp} number of average deep cycling days of deep cycling unit per year

E_{cur} maximum allowed curtailed wind energy

$E_{\text{dp}}^{(av)}$ average deep cycling energy per day of deep cycling unit

L_t predicted load at time t

$P_i^{\max}$ maximum power of normal unit or deep cycling unit

$P_i^{\min}$ minimum power of normal unit

P_j^{nomin} minimum power of deep cycling unit j in normal operation area

P_j^{dpmin} minimum power of deep cycling unit j in deep cycling area

$P_{\text{tie},t}^{\text{plan}}$ original tie line plan at time t

$R_i^{\text{up,max}}$ maximum upward reserve of normal unit i

$R_i^{\text{up,min}}$ minimum upward reserve of normal unit i

$R_i^{\text{dn,max}}$ maximum downward reserve of normal unit i

$R_i^{\text{dn,min}}$ minimum downward reserve of normal unit i

$R_{\text{sysup},t}$ upward reserve demand of the system at time t

$R_{\text{sysdn},t}$ downward reserve demand of the system at time t

$R_{\text{wup},t}$ upward reserve demand of the wind power at time t

$R_{\text{wdn},t}$ downward reserve demand of the wind power at time t

S_{dp} generation capacity of deep cycling unit

T number of dispatch intervals

ΔT time interval

$\overline{T}_k$ capacity of line k

$W_{\mathrm{for}n,t}$ predicted wind power of wind power plant n at time t

$\underline{W_{\mathrm{err}n,t}}$ lower bound of the prediction interval of the n^{th} wind power plant

$\overline{W_{\mathrm{err}n,t}}$ upper bound of the prediction interval of the n^{th} wind power plant

b_{om} annual operation & maintenance cost per unit of deep cycling unit

$c_{\mathrm{dp}j}$ unit cost of deep cycling unit j in deep cycling area

$c_{\mathrm{w}n}$ unit cost of the wind power curtailment of wind farm n

$k_{i,t}^{\mathrm{up}}$ unit cost of upward spinning reserve of normal unit i at time t

$k_{i,t}^{\mathrm{dn}}$ unit cost of downward spinning reserve of normal unit i at time t

$r_{i,\mathrm{up}}$ upward regulation rate of unit i

$r_{i,\mathrm{dn}}$ downward regulation rate of unit i

ρ lifespan reduction factor of deep cycling unit

Variables

$P_{i,t}$ generation scheduling of normal unit i at time t

$P_{k,t}$ power of line k at time t

$R_{i,t}^{\mathrm{up}}$ upward reserve of normal unit i at time t

$R_{i,t}^{\mathrm{dn}}$ downward reserve of normal unit i at time t

$W_{\mathrm{sche}n,t}$ scheduled wind power output of the wind power plant n at time t

$\delta P_{j,t}^{(d)}$ magnitude between P_j^{nomin} and P_j^{dpmin} at time t

$\delta P_{j,t}^{(n)}$ magnitude between P_j^{max} and P_j^{nomin} at time t

RE modelling

Parameters

$\Delta P^{\mathrm{RE}}_{\mathrm{EPAC},t}$ excessive power accommodation capability of the RE at time t

$P^{\mathrm{RE}}_{i,t}$ optimized power output of normal unit i from RE modelling

k_h parameter of the slight adjustment

ASE modelling

Objective functions

ΔC_{ASE} adjusted total cost of the SE

ΔC_{cur} adjusted cost of the wind power curtailment of the SE

ΔC_{gnom} adjusted cost of normal units in SE

ΔC_{dnom} adjusted normal status cost of the deep cycling units in SE

ΔC_{dcyc} adjusted deep cycling cost of the deep cycling units in SE

ΔC_{tie} adjusted cost for the tie line plan adjustment

Parameters

P_{TTC} total transfer capability of tie line

$P^{\mathrm{SE}}_{i,t}$ optimized power output of normal unit i from SE modelling

$P^{\mathrm{SE}}_{k,t}$ power of line k at time t from SE modelling

$W^{\mathrm{SE}}_{\mathrm{sche}n,t}$ scheduled wind power output of the wind power plant n at time t from SE modelling

c_{tie} unit cost of tie line power adjustment

$c_{\mathrm{dnom},j}$ unit cost of deep cycling unit j in normal area

$c_{\mathrm{gnom},i}$ unit cost of power adjustment of normal unit i

t_{start} the time interval when wind power curtailment first occurs in dispatch results of SE modelling

t_{end} the time interval when wind power curtailment last occurs

$\delta P_{j,t}^{\text{SE}(d)}$ optimized $\delta P_{j,t}^{(d)}$ of normal unit i from SE modelling

$\delta P_{j,t}^{\text{SE}(n)}$ optimized $\delta P_{j,t}^{(n)}$ of deep cycling unit j from SE modelling

λ_{ik} branch flow sensitivity with respect to normal unit i

λ_{jk} branch flow sensitivity with respect to deep cycling unit j

λ_{nk} branch flow sensitivity with respect to wind farm n

Variables

$\Delta P_{i,t}$ adjusted generation scheduling of normal unit i at time t

$\Delta P_{j,t}^{(d)}$ adjusted magnitude between P_j^{nomin} and P_j^{dpmin} at time t

$\Delta P_{j,t}^{(n)}$ adjusted magnitude between $P_j^{\max}$ and P_j^{nomin} at time t

$\Delta W_{\text{sche}n,t}$ adjusted scheduled wind power output of the wind power plant n at time t

$\Delta P_{\text{tie},t}$ adjusted tie line plan

ARE modelling

Objective functions

ΔC_{ARE} adjusted total cost of the RE

Parameters

$\Delta P_{\text{tie},t}^{\text{ASE}}$ optimized tie line power adjustment from ASE modelling

Other Parameters

$C_{\text{a}}^{(D)}$ accumulated cost of wind power curtailment and deep cycling within D days

$C_{\text{as}}^{(D)}$ accumulated cost of wind power curtailment, deep cycling and start-up of coal units within D days

$C_{\text{cur}}^{(d)}$ cost of the wind power curtailment in d^{th} day

$C_{\text{dcyc}}^{(d)}$ deep cycling cost in d^{th} day

C_s start-up cost of coal units

D number of operation days

1 Introduction

1.1 Motivation and aims

Emission-free power generation and sustainable energy supply are two key benefits of the wind power. With the increase of wind power penetration [1], the anti-correlation between wind power and system demand increases the operation pressure of the system [2, 3]. For systems with high wind penetration, evidences show that the operation flexibility is sensitive to wind power fluctuations during the valley load periods for systems with coal-fired units as the dominant generators (e.g. Colorado in the USA, Germany, Poland and China) [4-6]. As wind power generation may be very high during the valley load period, in order to maintain the power balance, power output of coal units in these systems may experience "deep cycling" [4]. In deep cycling status, the power level of coal units is below their normal minimum bound, and the operation cost is very high due to increased plant maintenance and reduced plant lifespan.

Long start-up time, high start-up cost and high minimum power output are key features of coal fired units. Unlike short start-up time of gas turbine units, the cold start-up time of coal units is around 20 hours or even longer. Meanwhile, the minimum shut-down time of coal units also takes several hours, which further extends the out-of-service state of coal units [7, 8]. Besides, coal units in these systems often have very large capacities and they cannot be shut down flexibly. Further, the start-up costs of coal units are extremely high and significantly affect the overall operational costs of the system. Such features force coal units to be scheduled in a 72-hour residual unit commitment (UC) or weekly UC [9, 10]. That is to say, UC of coal units can be seen as *fixed* for day ahead scheduling. Hence, power systems with coal-fired units as major generators lack the capability to cope with large wind power variance, and such systems are also described as Wind-Coal Intensive Systems (WCIS).

Generally speaking, WCIS are always connected with other load centers by long distance transmission lines [11] as most wind farms are often far away from the load centers. Such interconnected power systems have some distinctive characteristics as the sending end system is the WCIS and the receiving end system is a load center, and these multi-area systems are named as interconnected WCIS (IWCIS) which exist in the USA, China and other countries [6, 12]. Similar to conventional interconnected systems that can procure reserve assistance from neighboring areas [13], WCIS can also acquire assistance from the load center for accommodating excessive wind power. However, as the original tie line plans are often implemented through contracts that are strictly followed by regional systems [14], the coordination of WCIS may experience severe inflexibility along with the rapid increase of wind power generations.

This paper primarily aims to establish an optimal dispatch model of WCIS which considers both the wind power curtailment and deep cycling of coal units. Based on the optimized dispatch results of each regional system, the tie line plan adjustment strategy of IWCIS is proposed. The tie line power adjustment strategy aims at relieving deep cycling and wind curtailment of WCIS by exploiting surplus generation capacity from the load center.

1.2 Literature review and contributions

Various issues regarding wind power accommodation and multi-area system coordination can be found in many existing publications. For wind power accommodation, Wang *et al.* [5] demonstrated that coal units cannot provide a favorable environment for accommodating variable wind generation. Albadi [15] concluded that higher integration costs can be incurred due to the intermittent nature of the wind power. Chang et al. [16] proposed a new optimal power flow algorithm and revealed that wind generation systems will affect the bus voltage and transmission losses. Chun [17] proved that wind power curtailment may reduce system operation cost significantly. Doherty et al. [18] studied the impact of wind power on the system operation cost and the carbon emissions of the Irish system dominated by gas generation. For multi-area system operation, Khatir et al. [13] proposed an augmented Lagrangian algorithm to optimally schedule the generating units of multi-area systems. Ying et al. [14] proposed an approach to incorporate contracts into multi-area UC solutions, and coal units were treated as "must-run" generators due to their long start-up time. Chung et al. [19] utilized Benders decomposition to deal with multi-area unit commitment problems. Soroudi and Rabiee [20] proposed a multi-area dynamic economic dispatch model, taking into account wind power generation and power pool market to supply the overall demand of the system for a given horizon. Abdullah et al. [21] developed a wind resource sharing strategy for an interconnected system to achieve the national and regional renewable energy target.

Although the impact of wind power on the regional system operation has been intensively researched, distinctive operation features of WCIS are barely discussed in the literature. These features include:

(i) The UC of WCIS can be seen as fixed as the start-up cost of coal units is usually high while the start-up time of coal units is very long.

(ii) Wind power curtailment and deep cycling of coal units are very likely to occur.
(iii) Unit cost of deep cycling is extremely higher than other unit operation costs.

The operation feature (i) indicates that 0/1 binary variables for describing the start-up/shut-down statuses of coal units in conventional UC models can be avoided in the optimal scheduling of WCIS. For operation feature (ii), as the deep cycling status and the normal operational status of coal units are different, this operation feature may lead to a mixed integer problem. Operation feature (iii) indicates that reducing deep cycling should be in a primary aim in the day-ahead dispatch model of WCIS.

Ideally, the grid operator could centrally regulate all the interconnected systems. However, in reality, due to various political, economical and technical reasons, such operations are rarely implemented for multi-area systems as the operational independence is a distinctive feature of the interconnected systems [13]. Generally, a tie line power plan of a multi-area system is often made based on the obligation contracts and is strictly implemented by regional systems during the whole system operation. Thus, it is rather difficult to achieve the global optimality of the operation cost of interconnected power systems [22].

In this paper, the economic dispatch model and tie line plan adjustment strategy are proposed, which take into account of the distinctive operation characteristics of IWCIS, distinctively from existing approaches. We propose a deep cycling model that can avoid the 0/1 problems in economic dispatch. Further, we propose two measures for the tie line power adjustment during valley load periods, namely the timing window and excessive power accommodation capability (EPAC) of the load center, which both help IWCIS to accommodate large penetration of wind power.

The remaining paper is organized as follows. Section 2 discusses the operation characteristics of WCIS and the decompositions of IWCIS. Section 3 details the

WCIS modelling, and proposes the new tie line plan adjustment strategy. Section 4 presents case studies of a typical IWCIS to confirm the efficacy of the proposed strategy. Conclusions and discussions are given in Section 5.

2 Mechanism of tie line power adjustment of IWCIS

2.1 Operation characteristics of WCIS during valley load periods

Wind power plants are often given high priority in generating power, and the price of wind power is legally allowed to be higher than normal price of electricity generated by coal units [23]. For coal units, the unit cost of deep cycling is usually much higher than that of wind power. In this paper, all unit costs are based on the current electric price policy of China [5]. Deep cycling is a very special operational status for coal units, it is only applied to maintain the power balance, and coal units in deep cycling status do not participate in offering spinning reserve during valley load periods. It should also be noted that not all coal units take part in deep cycling regulation.

The anti-correlation between wind power and load during off-peak periods is illustrated in Fig. 1. The load and wind power data used in this paper is extracted from a typical WCIS in Northern China. Generation equipment and power output statistics of the WCIS are shown in Table 1.

In Fig. 1, during the valley load period, the minimum net load of the WCIS is around 4600 MW. Neglecting the effect of energy storage systems, the normal minimum power output of coal units is 840 MW higher than the minimum net load. To maintain the power balance, wind power curtailment is required first until the generated wind power reaches the maximum limit, then deep cycling of coal units is adopted later to ride through the valley load period. It is clear that the coal units will be forced to operate in a more stressed-out deep cycling mode after the nuclear units are put into operation.

From the optimization point of view, as the cost of deep cycling of coal units is extremely higher than other operation costs of generation units, deep cycling would be the last measure for the system to keep the power balance, and reducing the deep cycling cost should be given a high priority in minimizing the operation cost of WCIS during optimization. As wind power curtailment and deep cycling have significant impact on the operation cost of WCIS, it is obvious that the time periods for both wind power curtailment and deep cycling are the key time durations that WCIS can procure assistance from the connected load center.

2.2 Decomposition of IWCIS

A simplified topology of IWCIS is shown in Fig. 2.Based on Fig. 2, the generation scheduling of IWCIS can be formulated as the following steps:

(1) As the original tie line power plans are made based on the energy contracts and can be seen as a constant in a relatively long time interval, the sending end system and receiving end system can be treated as two isolated regional power systems, thus the model of the sending end system (SE) and the model of the receiving end system (RE) can be established independently.

(2) Based on the optimized result of the SE model, the wind power curtailment and deep cycling power of coal units in the SE model can be obtained. Meanwhile, the excessive power accommodation capability (EPAC) of the RE can also be calculated from the RE model.

(3) Based on the time duration of the wind power curtailment or deep cycling in the SE model, the timing window for the tie line power adjustment of WCIS can then be calculated, and the power adjustment of the tie line can only be implemented in this timing window.

(4) During the timing window for the tie line power adjustment, the power adjustment model of the SE (ASE) can be established. The objective of this model is to reduce both the wind power curtailment and the deep cycling of the units in the SE. Meanwhile, the obtained power adjustment of the tie line in ASE model is also restricted by EPAC of the RE. The adjusted power of the tie line reflects the reduction of the wind power curtailment and deep cycling.

(5) Once the tie line power adjustment is obtained from the ASE model, the optimal power adjustment model for the RE (ARE) can be established. The objective of the ARE model is to minimize the adjusted operation cost of the RE with the adjusted tie line power.

The flow chart of the strategy is shown in Fig. 3, where two decompositions are applied in the modelling process, namely the decomposition of SE and RE, and the decomposition of ASE and ARE. The first decomposition is based on the operation independence and contract obligation between two regional systems. The second decomposition follows two steps, the first step is to achieve EPAC of the RE, and the second step is to send the tie line adjustment information from SE back to the RE . The information interchange in this process is concise which fully considers the operation independence of regional systems.

3 Modelling of IWCIS

3.1 Deep Cycling Modelling

The power output characteristics of coal units with deep cycling capability are shown in Fig. 4.

As shown in Fig. 4, once the power output of the coal units is lower than P^{nomin}, the coal units will be operated in the deep cycling status.

The unit cost of the deep cycling unit c_{dp} is set as follows:

$$c_{\mathrm{dp}} = \frac{b_{\mathrm{om}} S_{\mathrm{dp}} \rho}{E_{\mathrm{dp}}^{(av)} D_{\mathrm{dp}}} \tag{1}$$

Parameters in (1) can be obtained from retired coal units that were involved in deep cycling. c_{dp} is extremely high due to the lifespan reduction of deep cycling generators, which is reflected by ρ.

In Fig. 4, P^{nomin} can be seen as a bound to distinguish the normal operation status from the deep cycling status. To avoid solving a mixed integer problem in deep cycling modelling, two continuous variables $\delta P^{(d)}$ and $\delta P^{(n)}$ which fully exploit the significant difference between c_{dp} and c_{gnom} are defined in the deep cycling modelling, as shown in Fig. 4. It should be noted that $\delta P^{(d)}$ and $\delta P^{(n)}$ are not variables to represent the actual power outputs of the coal units, but instead they are variables to describe the magnitude differences between power limits of coal units. From Fig. 4, the power limits of $\delta P^{(n)}$ and $\delta P^{(d)}$ are:

$$\begin{cases} 0 \le \delta P^{(n)} \le P^{\max} - P^{\mathrm{nomin}} \\ 0 \le \delta P^{(d)} \le P^{\mathrm{nomin}} - P^{\mathrm{dpmin}} \end{cases} \tag{2}$$

The total operation cost of the deep cycling unit C_{tot} is:

$$\begin{aligned} & C_{\mathrm{tot}} = C_{\mathrm{dnom}} + C_{\mathrm{dcyc}} \\ & \begin{cases} C_{\mathrm{dnom}} = f_{\mathrm{dnom}}(P^{\mathrm{nomin}} + \delta P^{(n)}) \\ C_{\mathrm{dcyc}} = c_{\mathrm{dp}}(P^{\mathrm{nomin}} - P^{\mathrm{dpmin}} - \delta P^{(d)}) \end{cases} \end{aligned} \tag{3}$$

In (3), the deep cycling level of the coal power plant is denoted by the difference between P^{nomin} and $P^{\mathrm{dpmin}}+\delta P^{(d)}$. Bigger difference implies severer deep cycling operation.

Assume the objective of the SE model is set to minimize the operation cost of the SE. As c_{dp} is much higher than the costs of other generation units, avoiding deep cycling is the primary target in the objective optimization. If wind power output is not high and the dispatch situation during the valley load period is not severe, the optimized result for $\delta P^{(d)}$ will be P^{nomin}-P^{dpmin} and $\delta P^{(n)}$ will be greater than zero. On the contrary, if the wind power is high and deep cycling units tend to operate in the deep cycling mode during the valley load period, $\delta P^{(n)}$ will be reduced to 0 first due to the power balance constraint. Then P^{dpmin}+$\delta P^{(d)}$ will become smaller than P^{nomin} to maintain the power balance. Consequently, no matter a deep cycling unit is in normal status or in deep cycling status, the power output can both be expressed as:

$$P = P^{\text{dpmin}} + \delta P^{(d)} + \delta P^{(n)} \tag{4}$$

According to (4), P includes $\delta P^{(d)}$ and $\delta P^{(n)}$ and both variables are continuous, thus P can be optimized throughout while meeting all physical constraints in the WCIS modelling, and the mixed integer optimization problem is thus avoided.

3.2 Spinning reserve modelling of wind power

Empirical distribution function can be adopted to approximate the probability distribution of wind power prediction error. It is assumed that the future wind power prediction errors follow the same error probability distribution of historic prediction errors [24]. After the extreme forecasting errors are eliminated, the largest negative and positive prediction errors (e.g., values beyond 6 times of the standard deviation of the forecasting error) of the n^{th} wind power plant are denoted as [5]

$$\left\{(\underline{W_{\text{err}n,t}}, \overline{W_{\text{err}n,t}}), t = 1, 2, \ldots, T\right\} \tag{5}$$

The spinning reserve demand of the total wind power in SE can be then obtained by:

$$\begin{cases} R_{\text{wup},t} = \sum_{n \in \Omega_{\text{ws}}} \underline{W_{\text{err}n,t}} \\ R_{\text{wdn},t} = \sum_{n \in \Omega_{\text{ws}}} \overline{W_{\text{err}n,t}} \end{cases} \tag{6}$$

3.3 SE modelling and timing window for tie line power adjustment

The objective is given as follows:

$$\min \quad C_{\text{com}} = C_{\text{gnom}} + C_{\text{dnom}} + C_{\text{dcyc}} + C_{\text{res}} + C_{\text{cur}} \tag{7}$$

$$\begin{cases} C_{\text{gnom}} = \sum_{t=1}^{T} \sum_{i \in \Omega_{\text{gs}}} f_{\text{gnom},i}(P_{i,t}) \\ C_{\text{dnom}} = \sum_{t=1}^{T} \sum_{j \in \Omega_{\text{dps}}} f_{\text{dnom},j}(P_j^{\text{nomin}} + \delta P_{j,t}^{(n)}) \\ C_{\text{res}} = \sum_{t=1}^{T} \sum_{i \in \Omega_{\text{gs}}} (k_{i,t}^{\text{up}} R_{i,t}^{\text{up}} + k_{i,t}^{\text{dn}} R_{i,t}^{\text{dn}}) \\ C_{\text{dcyc}} = \sum_{t=1}^{T} \sum_{j \in \Omega_{\text{dps}}} c_{\text{dp}j}(P_j^{\text{nomin}} - P_j^{\text{dpmin}} - \delta P_{j,t}^{(d)}) \\ C_{\text{cur}} = \sum_{t=1}^{T} \sum_{n \in \Omega_{\text{ws}}} c_{\text{wn}}(W_{\text{forn},t} - W_{\text{schen},t}) \end{cases}$$

s.t.

$$\sum_{i \in \Omega_{\text{gs}}} P_{i,t} + \sum_{n \in \Omega_{\text{ws}}} W_{\text{schen},t} + \sum_{j \in \Omega_{\text{dps}}} (P_j^{\text{dpmin}} + \delta P_{j,t}^{(d)} + \delta P_{j,t}^{(n)}) = L_t + P_{\text{tie},t}^{\text{plan}} \tag{8}$$

$$\sum_{t=1}^{T} \sum_{n \in \Omega_{\text{ws}}} (W_{\text{forn},t} - W_{\text{schen},t}) \Delta T \le E_{\text{cur}} \qquad n \in \Omega_{\text{ws}} \tag{9}$$

$$W_{\text{schen},t} \le W_{\text{forn},t} \qquad n \in \Omega_{\text{ws}} \tag{10}$$

$$P_i^{\min} \le P_{i,t} \le P_i^{\max} \qquad i \in \Omega_{\text{gs}} \tag{11}$$

$$0 \le \delta P_{j,t}^{(d)} \le P_j^{\text{nomin}} - P_j^{\text{dpmin}} \qquad j \in \Omega_{\text{dps}} \tag{12}$$

$$0 \le \delta P_{j,t}^{(n)} \le P_j^{\max} - P_j^{\text{nomin}} \qquad j \in \Omega_{\text{dps}} \tag{13}$$

$$-r_{i,\text{dn}} \Delta T \le P_{i,t} - P_{i,t-1} \le r_{i,\text{up}} \Delta T \qquad i \in \Omega_{\text{gs}} \tag{14}$$

$$-r_{j,\text{dn}} \Delta T \le (P_j^{\text{dpmin}} + \delta P_{j,t}^{(d)} + \delta P_{j,t}^{(n)}) - (P_j^{\text{dpmin}} + \delta P_{j,t-1}^{(d)} + \delta P_{j,t-1}^{(n)}) \le r_{j,\text{up}} \Delta T \qquad j \in \Omega_{\text{dps}} \tag{15}$$

$$\left| P_{k,t} \right| \le \overline{T}_k, \qquad k \in \Omega_{\text{bs}} \tag{16}$$

$$\begin{cases} \sum_i R_{i,t}^{\text{up}} \ge R_{\text{sysup},t} + R_{\text{wup},t} \\ P_{i,t} + R_{i,t}^{\text{up}} \le P_i^{\max} \\ R_i^{\text{up,min}} \le R_{i,t}^{\text{up}} \le R_i^{\text{up,max}} \end{cases} \qquad i \in \Omega_{\text{gs}} \tag{17}$$

$$\begin{cases} \sum_i R_{i,t}^{\text{dn}} \ge R_{\text{sysdn},t} + R_{\text{wdn},t} \\ P_{i,t} - R_{i,t}^{\text{dn}} \ge P_i^{\min} \\ R_i^{\text{dn,min}} \le R_{i,t}^{\text{dn}} \le R_i^{\text{dn,max}} \end{cases} \qquad i \in \Omega_{\text{gs}} \tag{18}$$

The objective in (7) minimizes the operation cost of normal coal units, deep cycling units, spinning reserve procurement and wind power curtailment. Equation (8) is the power balance constraint for WCIS. Equations (9) and (10) are the constraints for the maximum wind power curtailment and the maximum scheduled wind power, respectively. Equations (11-13) are the power output bounds of normal coal units and deep cycling units, respectively. Equations (14) and (15) model the ramping constraints of normal units and deep cycling units, respectively. Equation (16) models the maximum limits of branch line flows. Equations (17) and (18) model the constraints of upward and downward spinning reserves, respectively.

By solving the SE model, the optimized dispatch results for $P_{i,t}^{\mathrm{SE}}$, $W_{\mathrm{sche}n,t}^{\mathrm{SE}}$, $\delta P_{j,t}^{\mathrm{SE}(d)}$ and $\delta P_{j,t}^{\mathrm{SE}(n)}$ can be achieved. According to the SE modelling analysis in Section 3.1, if $\delta P_{j,t}^{\mathrm{SE}(n)}>0$, then $\delta P_{j,t}^{\mathrm{SE}(d)}=P_j^{\mathrm{nomin}}-P_j^{\mathrm{dpmin}}$. Under this circumstance, the corresponding coal unit is operated in the normal operational region. However, if $\delta P_{j,t}^{\mathrm{SE}(n)}=0$, then $\delta P_{j,t}^{\mathrm{SE}(d)}\leq P_j^{\mathrm{nomin}}-P_j^{\mathrm{dpmin}}$, which implies deep cycling occurs in the SE model.

Suppose that the first time interval when wind power curtailment occurs according to the dispatching results of the SE model is denoted as t_{start}, and the time interval when the last wind power curtailment occurs is denoted as t_{end}, then the timing window for the tie line power adjustment can be set as [t_{start}, t_{end}].

3.4 RE modelling and calculation of EPAC

The RE modelling has the same procedure as the SE modelling, but the deep cycling and wind power curtailment are both neglected in the RE modelling due to high load level in the load center. Based on the optimized results of RE, the EPAC of the RE ($\Delta P_{\mathrm{EPAC},t}$) is given as:

$$\Delta P_{\mathrm{EPAC},t}^{\mathrm{RE}}=\sum_{i\in\Omega_{\mathrm{gr}}}\min(P_{i,t}^{\mathrm{RE}}-P_i^{\mathrm{min}},k_h r_{i,\mathrm{dn}}\Delta T) \tag{19}$$

The EPAC reflects downward generation space in the load center. Generally, load centers with larger generation capacity have a stronger EPAC to accommodate wind power from the WCIS.

3.5 ASE Modelling

Within the whole time intervals [t_{start}, t_{end}], the ASE modelling is formulated as the following maximization problem,

$$\max \quad \Delta C_{\text{ASE}} = \Delta C_{\text{cur}} + \Delta C_{\text{dcyc}} - \Delta C_{\text{gnom}} - \Delta C_{\text{dnom}} - \Delta C_{\text{tie}} \tag{20}$$

$$\begin{cases} \Delta C_{\text{cur}} = \sum_{t=t_{\text{start}}}^{t_{\text{end}}} \sum_{n\in\Omega_{\text{ws}}} c_{\text{w}n} \Delta W_{\text{sch}en,t} \\ \Delta C_{\text{dcyc}} = \sum_{t=t_{\text{start}}}^{t_{\text{end}}} \sum_{j\in\Omega_{\text{dps}}} c_{\text{dp}j} \Delta P_{j,t}^{(d)} \\ \Delta C_{\text{gnom}} = \sum_{t=t_{\text{start}}}^{t_{\text{end}}} \sum_{i\in\Omega_{\text{gs}}} c_{\text{gnom}i} \Delta P_{i,t} \\ \Delta C_{\text{dnom}} = \sum_{t=t_{\text{start}}}^{t_{\text{end}}} \sum_{j\in\Omega_{\text{dps}}} c_{\text{dnom}j} \Delta P_{j,t}^{(n)} \\ \Delta C_{\text{tie}} = \sum_{t=t_{\text{start}}}^{t_{\text{end}}} c_{\text{tie}} \Delta P_{\text{tie},t} \end{cases}$$

s.t.

$$\sum_{i\in\Omega_{\text{gs}}} \Delta P_{i,t} + \sum_{i\in\Omega_{\text{dps}}} (\Delta P_{j,t}^{(d)} + \Delta P_{j,t}^{(n)}) + \sum_{n\in\Omega_{\text{ws}}} \Delta W_{\text{sch}en,t} - \Delta P_{\text{tie},t} = 0 \tag{21}$$

$$0 \le \Delta P_{i,t} \le \min(P_i^{\max} - P_{i,t}^{\text{SE}}, k_h r_{i,\text{up}} \Delta T) \qquad i \in \Omega_{\text{gs}} \tag{22}$$

$$0 \le \Delta P_{j,t}^{(d)} \le \min(P_j^{\text{nomin}} - P_j^{\text{dpmin}} - \delta P_{j,t}^{\text{SE}(d)}, k_h r_{j,\text{up}} \Delta T)\, j \in \Omega_{\text{dps}} \tag{23}$$

$$0 \le \Delta P_{j,t}^{(n)} \le \min(P_j^{\max} - P_j^{\text{nomin}} - \delta P_{j,t}^{\text{SE}(n)}, k_h r_{j,\text{up}} \Delta T)\, j \in \Omega_{\text{dps}} \tag{24}$$

$$0 \le \Delta W_{\text{sch}en,t} \le W_{\text{for}n,t} - W_{\text{sch}en,t}^{\text{SE}} \tag{25}$$

$$\begin{aligned} &\sum_{i\in\Omega_{\text{gs}}} \lambda_{ik} \Delta P_{i,t} + \sum_{j\in\Omega_{\text{dps}}} \lambda_{jk} (\Delta P_{j,t}^{(d)} + \Delta P_{j,t}^{(n)}) + \sum_{n\in\Omega_{\text{ws}}} \lambda_{nk} \Delta W_{\text{sch}en,t} \\ &\qquad \le \overline{T}_k - P_{k,t}^{\text{SE}}, k \in \Omega_{\text{bs}} \end{aligned} \tag{26}$$

$$0 \le \Delta P_{\text{tie},t} \le \min\{P_{\text{TTC}} - P_{\text{tie},t}^{\text{plan}}, \Delta P_{\text{EPAC},t}^{\text{RE}}\} \tag{27}$$

The objective in (20) maximizes the cost reduction. Note that $c_{\text{dp}j} >> c_{\text{w}n} > c_{\text{tie}} > \max\{c_{\text{gnom}i}, c_{\text{dnom}j}\}$ and that ΔC_{tie} is the cost for the tie line plan adjustment, which reflects the operation independence of interconnected power systems. Equation (21) is the constraint of the adjusted power balance. Equations (22) to (24) are the constraints of the adjusted power of normal units and the deep cycling units, respectively. $P_{i,t}^{\mathrm{SE}}$, $\delta P_{j,t}^{\mathrm{SE}(d)}$ and $\delta P_{j,t}^{\mathrm{SE}(n)}$ in these equations, are all obtained from the SE modelling. Equation (25) is the constraint of wind power adjustment. Equation (26) models the branch line overloading. Equation (27) is the limits of the tie line power adjustment.

In (20), the objective of the ASE modelling is to reduce the wind power curtailment and deep cycling in WCIS by adjusting the tie line plan, while the adjustment of the tie line plan incurs a cost. In Equations (23) and (24), if $\delta P_{j,t}^{\mathrm{SE}(d)} = P_j^{\mathrm{nomin}} - P_j^{\mathrm{dpmin}}$ in the SE modelling, then $\Delta P_{j,t}^{(d)}$ =0. If $\delta P_{j,t}^{\mathrm{SE}(d)} \le P_j^{\mathrm{nomin}} - P_j^{\mathrm{dpmin}}$, then $\Delta P_{j,t}^{(d)}$ is the optimized result which implies that the deep cycling of coal units in WCIS is reduced after the tie line plan adjustment.

The optimized result $\Delta P_{\mathrm{tie},t}$ ($\Delta P_{\mathrm{tie},t}^{\mathrm{ASE}}$) in the ASE modelling will be sent back to the load center for ARE modelling.

3.6 ARE Modelling

The objective of the ARE model is:

$$\min \quad \Delta C_{\mathrm{ARE}} = \sum_{t=t_{\mathrm{start}}}^{t_{\mathrm{end}}} \sum_{i\in\Omega_{\mathrm{gr}}} c_{\mathrm{gnom}i}(-\Delta P_{i,t}) \tag{28}$$

s.t.

$$\sum_i \Delta P_{i,t} = -\Delta P_{\mathrm{tie},t}^{\mathrm{ASE}} \quad i\in\Omega_{\mathrm{gr}} \tag{29}$$

$$\max(P_i^{\min} - P_{i,t}^{\mathrm{RE}}, -k_h r_i \Delta T) \le \Delta P_{i,t} \le 0 \quad i\in\Omega_{\mathrm{gr}} \tag{30}$$

In (30), $P_{i,t}^{\mathrm{RE}}$ and $\Delta P_{\mathrm{tie},t}^{\mathrm{ASE}}$ are obtained from the RE modelling and ASE modelling, respectively.

3.7 System performance indices

Under certain operational circumstances, shutting down a few coal units may mitigate the wind power curtailment and deep cycling of coal units during the valley load period. However, this is based on paying extremely high shut-down cost of coal units [7]. To evaluate the benefit of shutting down coal units in WCIS, the following system indices related to the long-term operation cost are adopted for system performance analysis.

1) *Accumulated cost of wind power curtailment and deep cycling of coal units*

$$C_{\mathrm{a}}^{(D)} = \sum\nolimits_{d=1}^{D} \{C_{\mathrm{cur}}^{(d)} + C_{\mathrm{dcyc}}^{(d)}\} \tag{31}$$

2) *Accumulated cost of wind power curtailment, deep cycling and start-up of coal units*

$$C_{\mathrm{as}}^{(D)} = C_{\mathrm{s}} + \sum\nolimits_{d=1}^{D} \{C_{\mathrm{cur}}^{(d)} + C_{\mathrm{dcyc}}^{(d)}\} \tag{32}$$

If $C_{\mathrm{as}}^{(D)} < C_{\mathrm{a}}^{(D)}$, then shutting down coal units would be more beneficial in the long term than maintaining these units in operation.

4 Case study

4.1 System parameters

The modified Dongbei system (DB) is a WCIS [25] with 9 normal coal units, 2 deep cycling coal units and 3 wind farm clusters. To focus on the interactions between wind power and coal units in the DB system, the energy storage system in [25] is replaced by a coal unit. While the Huabei system (HB) is a simplified load center with 23 coal units. Both DB and HB are connected by a 500 kV transmission line, forming a typical IWCIS. The installed generation capacities of DB are shown in Table 2. The wind power penetration level in DB is 13.2%, which is rather high for a WCIS. The original day ahead tie line plan is shown in Table 3. The dispatch interval is 15 minutes. Parameters for the coal units and wind farm clusters in the DB system are shown in Table 4. Parameters for the coal units in HB are similar to those in DB due to the same generation type. The simplified geographical layout of the DB and HB is shown in Fig. 5. The predicted load and wind power curve for the DB (from intervals 1 to 48) are shown in Fig. 6. The allowed maximum curtailed wind energy E_{cur} for a single day for DB is 800 MWh. The unit cost of the curtailed wind power (c_{w}) and deep cycling (c_{dp}) are 1.1×10^2\$/MWh and 2.3×10^2\$/MWh, respectively. The spinning reserve demand of the system ($R_{\text{sysup},t}$, $R_{\text{sysdn},t}$) and that of wind power ($R_{\text{wup},t}$, $R_{\text{wdn},t}$) in DB are 170 MW and 50 MW in each dispatch interval, respectively.

4.2 Day ahead dispatch result of system DB and HB

The economic dispatch of DB and HB are calculated by the SE and RE models, respectively. The dispatch result for DB during the valley load period is shown in Table 5. It is noted that the curtailed wind power from the wind farm rather than the scheduled power is shown in Table 5. To demonstrate the deep cycling level, $\delta P^{(d)}$ and $\delta P^{(n)}$ of G10 and G11 are also shown.

According to the dispatched results, both wind power curtailment and deep cycling occur within the time intervals from 7 to 24. During these intervals, G2, G3 and G9 all work at the minimum power output, while G1, and G4 to G8 work above the minimum level to satisfy the downward reserve demand. In Table 5, the total curtailed wind power is 800 MWh which already reaches its maximum limit. Both wind power curtailment and deep cycling of unit G10 occur at the same time. Besides, $\delta P^{(d)}$ of G10 are all smaller than 260 MW and $\delta P^{(n)}$ of G10 are all 0 MW during the time intervals from 7 to 24 (i.e. power output of G10 is lower than 860 MW). Meanwhile, $\delta P^{(d)}$ of G11 is 200 MW and $\delta P^{(n)}$ is 0 MW (i.e. power output of unit G11 is 900 MW). These results substantiate the discussions in Section 3.1. Accordingly, deep cycling occurs for unit G10 during the time intervals between 7 and 24, and G11 maintains the critical normal operation status during these intervals, resulting in 232 MWh deep cycling. During the time intervals from 7 to 24, the total operation cost of wind power curtailment and deep cycling is 1.41×10^5\$. Though deep cycling energy is only 0.29 times of the curtailed wind energy, the operation cost of the deep cycling is 0.6 times of the wind power curtailment.

From Table 5, it can be seen that the time intervals from 7 to 24 with wind power curtailment and deep cycling is a specific time for all generation units in DB. Then the timing window for the tie line plan adjustment is also set for the time intervals from 7 to 24. To illustrate the relationship between wind power curtailment and deep cycling during these intervals, deep cycling power of G10 and curtailment of the wind farms in DB during intervals 7 to 24 are shown in Fig. 7.

In Fig. 7, the deep cycling curve of the G10 has strong correlation with the wind power curtailment. At the beginning of the valley load period, as the load level decreases, the deep cycling and wind power curtailment keep increasing. At interval 17, both the deep cycling power and curtailed wind power reach the maximum value because the net load of DB reaches its minimum level. Later with the recovery of the valley load, both deep cycling power and curtailed wind power keep decreasing and finally return to 0.

Comparatively, due to the high load level characteristics of the load center, wind power curtailment and deep cycling barely exist in HB. Thus, the dispatch pressure of HB is much less than DB, and HB has the capability to accept excessive power from DB. The EPAC of HB in the timing window is also shown in Table 5. It can be seen that the EPAC of HB varies at different time intervals. The reason is that the total power level of generation units has a strong correlation with the load variation.

During the valley load period the power output level of HB is also low because of its low load level, which introduces small $\Delta P_{\mathrm{EPAC},t}$ and reduces the capability of HB to accept excessive power from DB.

4.3 Tie line plan adjustment analysis

Once both SE and RE models are optimized, the power adjustment of coal units and wind power plants in DB can be achieved by optimizing the ASE model. Here, c_{tie} is set to 0.65×10^2\$/MWh in this case, which is higher than the cost of normal coal units in DB.

Results show that $\Delta P_{i,t}$ and $\Delta P_{j,t}^{(n)}$ are all 0 in the ASE modelling, which means that the tie line power adjustment is mainly utilized for the recovery of deep cycling power and wind power curtailment of DB. The reason is that the unit cost of tie line power adjustment c_{tie} is higher than $c_{\mathrm{gnom}i}$ and $c_{\mathrm{dnom}j}$, which blocks normal power adjustment of coal units in normal operational region. In fact, $\Delta P_{i,t}$ and $\Delta P_{j,t}^{(n)}$ have nonzero values only when the branch line congestion exists in the ASE model. Optimized adjustment of the tie line power is shown in Fig. 8, and recovery of deep cycling power and curtailed wind power in system DB is shown in Fig. 9.

From Fig. 8 and Fig. 9, compared with wind power curtailment, deep cycling power in DB is recovered in priority due to its extremely high cost. The adjusted power of G10 is equal to its deep cycling power in the SE model, which means that the deep cycling power of G10 is totally recovered after the tie line power adjustment. Meanwhile, during intervals 7 to 11 and intervals 22 to 24, the curtailed wind power in DB is totally recovered. However, during the intervals 12 to 21, wind power curtailment still exists due to the low level of EPAC of HB and the recovery priority of deep cycling power.

After the adjustment of the tie line plan, the deep cycling energy of G10 in DB is reduced to 0 and the total curtailed wind energy in DB is reduced to 366 MWh. The operation cost of DB is significantly reduced by 1.01×10^5\$, including 0.53×10^5\$ of deep cycling recovery of G10 and 0.48×10^5\$ of curtailed wind power recovery of wind farms. Meanwhile, the operational cost of HB is increased by 0.33×10^5\$ due to the power adjustment cost of coal units in HB.

4.4 Influence of wind power variance to the system operation during the valley load period

Suppose the wind power fluctuation is severe, which incurs an increase of the spinning reserve requirement, this will result in an increase of $R_{\mathrm{wdn},t}$ in DB by 20 MW at each dispatch interval.

Result shows that the power output of G1 is increased from 970 MW to 990 MW, providing more downward reserves to satisfy the spinning reserve demand of the wind power. Deep cycling power of G10 and total curtailed wind power in DB during interval 7 to 24 are shown in Fig. 10.

From Fig. 10, as the power output of G1 is increased by 20 MW, to maintain power balance, the total power output of G10 is forced to decrease, which means that the deep cycling power of G10 is increased at the same time. This reveals that severe wind power fluctuations with high spinning reserve demand during the valley load periods might lead to large deep cycling power of coal units. Meanwhile, the total curtailed wind power is also changed as the spinning reserve demand of the wind power increases. Consequently, the increase of the spinning reserve demand of the wind power is accommodated by the increase of the deep cycling power of G10 and the variations of wind power curtailment.

4.5 Analysis of shutting down coal units in system DB

To measure the impact of the shutting down coal units, a 10 day (weekday) long term generation scheduling of DB is investigated in this case, and the 1st day corresponds to the case study presented in Section 4.1. Two scenarios are considered in this case. In Scenario 1 (SC_1), all units in DB remain in operation. In Scenario 2 (SC_2), G8 whose generation capacity is the smallest (also with the shortest start-up time and lowest start-up cost) in DB is attempted to be shut-down at 0:00 in the 1st day. Other coal units with larger capacities are still kept in operation. Load variance is smooth over the 10 days. To simplify the analysis and emphasize the comparison between SC_1 and SC_2, tie line power adjustment strategy is not adopted in this case.

Daily wind energy variance, daily deep cycling cost and wind power curtailment cost of SC_1 is shown in Fig. 11.

According to Fig. 11, wind power also varies significantly over the 10 days. On the 7th day, the wind power generation is even close to zero. Generally, deep cycling costs and wind power curtailment costs have high correlation with wind energy variance, which reflects that larger scale wind power may cause severer deep cycling and wind power curtailment. It is also clear that wind power curtailment is adopted first to avoid deep cycling of coal units. For instance, although wind power curtailment exists from 2nd day to 8th day, the deep cycling cost in these days is 0. However, due to the very high wind power penetration in the 9th day and 10th day, deep cycling costs are very high because wind power curtailment already reaches its maximum limit in these days.

By shutting down G8, daily deep cycling cost and wind power curtailment cost of SC_2 with same wind power variance as in SC_1 is shown in Fig. 12.

As shown in Fig. 12, wind power curtailment costs and deep cycling costs of DB are significantly reduced compared with SC_1, and deep cycling costs in these 10 days are all 0. However, this is based on shutting down a coal unit with an extremely high start-up cost. To further analyze the economic impact of shutting down the coal unit, total operation costs and accumulated costs indices of SC_1 and SC_2 are illustrated in Fig. 13 and Fig. 14, respectively. In Fig. 13, the shutting down cost of G8 is not included in the total operation costs of SC_2.

Fig. 13 reveals the strong correlation of the total operation costs of SC_1 and SC_2 with the wind power variance. As G8 is kept in operation in SC_1, the curtailed wind power and deep cycling power is very high in day 9 and day 10 when the wind power penetration is high, causing much higher total operation costs of SC_1 than that of SC_2. By shutting down G8, the total operation cost during these days can be notably reduced. Fig. 14 shows that the C_a curve of SC_1 increases rapidly in the 9th and 10th days due to the extremely high deep cycling cost and wind power curtailment cost as shown in Fig 11. As C_{as} of SC_2 is higher than C_a of SC_1 in 1st day, shutting down G8 is not economic for this day. The reason is that a very high start-up cost of G8 greatly increases C_{as} of SC_2, incurring C_{as} of SC_2 higher than that of SC_1 in the 1st day. From the UC point of view, the results in Fig. 14 show that the impact of shutting down coal units should be reflected in a long time interval rather than day scale due to the high start-up cost, which greatly distinguishes UC of WCIS from other UC problems. Consequently, long start-up time and high start-up cost are both the main reasons to fix UC of coal units day ahead in WCIS.

5 Conclusions

An economic dispatch strategy that makes full use of the distinctive characteristics of IWCIS is proposed in this paper. Based on the distinctive operation features of WCIS, the special UC characteristics of WCIS are analyzed. Through a proper design of the optimization variables for deep cycling units in this economic dispatch model of WCIS, the mixed integer optimization problem is completely avoided. Case study results reveal that the model proposed in this paper can well illustrate the complicated interactions between the wind power curtailment and the deep cycling of coal units during valley load periods. It is shown that the impact of UC of WCIS can only be reflected in a longer time interval rather than over a day scale due to the extremely high start-up costs of coal units, and the wind power fluctuation in the long time interval has a strong correlation with the total operation cost of the system. Finally, shutting down coal units during valley load period might help reduce the deep cycling and wind power curtailment of coal units. The findings of this study can also be applied to interconnected systems where the RE is also a WCIS. However, such systems are not common and the wind power accommodation capacity of such systems is strongly restricted due to very weak EPAC of the RE.

6 Acknowledgements

This work is supported by EPSRC/NSFC jointly funded project 'Intelligent Grid Interfaced Vehicle Eco-charging (iGIVE)' under Grant (Nos. EP/L001063/1 and 51361130153), NSFC funded project under Grant No. 61533010 and China Postdoctoral Science Foundation (2013M540286).

References

[1] GWEC, 'Global Wind Energy Outlook' [Online]. Available: at http://www.gwec.net/index.php?id=181&L=pddbrgfhnvlkx, accessed June 2010

[2] Baldick, R.: 'Wind and energy markets: a case study of Texas', *IEEE Syst. Journal*, 2012, **6**, (1), pp. 27-31

[3] Aparicio, N., MacGill, I., Abbad, J., *et al.*: 'Comparison of wind energy support policy and electricity market design in Europe, the United States, and Australia',

IEEE Trans. Sust. Energy, 2012, **3**, (4), pp. 809–818

[4] Bentek Energy, ‘How Less Became More Wind, Power and Unintended Consequences in the Colorado Energy Market’ [Online]. Available at http://www.wind-watch.org/documents/wp-content/uploads/ BENTEK-How -Less - Became-More.pdf

[5] Wang, C., Lu, Z., Qiao, Y.: ‘A consideration of the wind power benefits in day-ahead scheduling of wind-coal intensive power systems’, *IEEE Trans. Power Syst.*, 2013, **28**, (1), pp. 236-245

[6] Rogers, K., Ragheb, M.: ‘Symbiotic coupling of wind power and nuclear power generation’. Proc. Int. Conf. 1st International Nuclear & Renewable Energy Conf. (INREC), Jordan, 2010

[7] Biskas, P., Baslis, C., Simoglou, C.: ‘Coordination of day-ahead scheduling with a stochastic weekly unit commitment for the efficient scheduling of slow-start thermal units’. Proc. Int. Conf. Symposium - Bulk Power System Dynamics and Control - VIII (IREP), Brazil, 2010

[8] U.S. Environmental Protection Agency, ‘Assessment of Startup Period at Coal-Fired Electric Generating Units’ [Online]. Available at http://www.epa.gov/mats/pdfs/matsstartstsd.pdf

[9] Simoglou, C., Biskas, P., Bakirtzis, A.: ‘Optimal self-scheduling of a thermal producer in short-term electricity markets by MILP’, *IEEE Trans. Power Syst.*, 2010, **25**, (4), pp. 1965-1977

[10] Price, J., Rothleder, M.: ‘Recognition of extended dispatch horizons in California’s energy markets’. Proc. Int. Conf. IEEE PES General Meeting, Detiort, USA, 2011

[11] Southern Hami-Zhengzhou UHVDC [Online]. Available at

http://en.wikipedia.org/wiki/Southern_Hami-Zhengzhou_UHVDC

[12] Aigner, T., Jaehnert, S., Doorman, G., *et al.*: 'The effect of large-scale wind power on system balancing in Northern Europe', *IEEE Trans. Sust. Energy*, 2012, **3**, (4), pp. 751–759

[13] Khatir, A., Conejo, A., Cherkaoui, R.: 'Multi-area unit scheduling and reserve allocation under wind power uncertainty', *IEEE Trans. Power Syst.*, 2014, **29**, (4), pp. 1701-1710

[14] Yingvivatanapong, C., Lee, W., Liu, E.: 'Multi-area power generation dispatch in competitive markets', *IEEE Trans. Power Syst.*, 2008, **23**, (1), pp. 196-203

[15] Albadi, M., Saadany, E.: 'Overview of wind power intermittency impacts on power systems', *Electr Power Syst Res*, 2010, **80**, (6), pp. 627-632

[16] Chang, Y., Lee, T., Chen, C., *et al.*: 'Optimal power flow of a wind-thermal generation system', *Int J Electr Power Energy Syst*, 2014, **55**, pp. 312-320

[17] Chun-Lung, C.: 'Optimal wind-thermal generating unit commitment', *IEEE Trnas. Energy Convers*., 2008, **23**, pp. 273-280

[18] Doherty, R., Outhred, H., O'Malley, M.: 'Establishing the role that wind generation may have in future generation protfolios', *IEEE Trans. Power Syst.*, 2006, **21**, (3), pp. 1415-1422

[19] Chung, K., Kim, B., Hur, D.: 'Multi-area generation scheduling algorithm with regionally distributed optimal power flow using alternating direction method', *Int. J. Electr. Power Energy Syst.*, 2011, **33**, (9), pp. 1527-1535

[20] Souroudi, A., Rabiee, A.: 'Optimal multi-area generation schedule cosidering renewable resources mix: a real-time approach', *IET Gener. Transm. Distrib.*, 2013, **7**, (9), pp. 1011–1026

[21] Abdullah, M., Muttaqi, K., Agalgaonkar, A., *et al.*: 'New approach for sharing

wind generation spatial diversification in multi-area power systems using trade-off analysis', *IET Gener. Transm. Distrib.*, 2014, **8**, (8), pp. 1466–1478

[22] U.S. Department of Energy, 'Analysis Methodology for Balancing Authority Cooperation in High Penetration of Variable Generation' [Online]. Available at http://www.pnl.gov/main/publications/external/technical_reports/PNNL-19229.pdf

[23] Yang, X., Song, Y., Wang, G., *et al.*: 'A comprehensive review on the development of sustainable energy strategy and implementation in China', *IEEE Trans. Sust. Energy*, 2010, **1**, (2), pp. 57–65

[24] Pinson, P.: 'Estimation of wind power forecast uncertainty' (Dissertation style), 2006, Ecole des Mines de Paris

[25] Wang, S., Yu, J.: 'Optimal sizing of the CAES system in a power system with high wind power penetration', *Int. J. Electr. Power Energy Syst.*, 2012, **37**, pp. 117-125

Figure Captions

Fig. 1 Typical load and wind power curve of a WCIS in Northern China.

Fig. 2 Simplified topology of IWCIS.

Fig. 3 Flow chart of the adjustment of tie line power plan.

Fig. 4 Deep cycling model of coal units for generation scheduling.

Fig. 5 Geographical diagram of the studied interconnected power system.

Fig. 6 Predicted load and wind power of DB during valley load period.

Fig. 7 Deep cycling power and wind power curtailment of system DB during valley load period.

Fig. 8 Optimal tie line power adjustment.

Fig. 9 Power adjustment of deep cycling and wind farm clusters.

Fig. 10 Deep cycling power of G10 and total curtailed wind power in DB when $R_{wdn,t}$ is 70 MW.

Fig. 11 Daily deep cycling cost and wind power curtailment cost of SC_1.

Fig. 12 Daily deep cycling cost and wind power curtailment cost of SC_2.

Fig. 13 Total operation cost of SC_1 and SC_2.

Fig. 14 Accumulated cost of SC_1 and SC_2.

Table Captions

Table 1 Generation equipment of WCIS in Northern China.

Table 2 Generating equipment and capacities of DB.

Table 3 Original day-ahead tie line plan.

Table 4 Parameters of coal units in system DB.

Table 5 Generation scheduling of the system DB during valley load period.

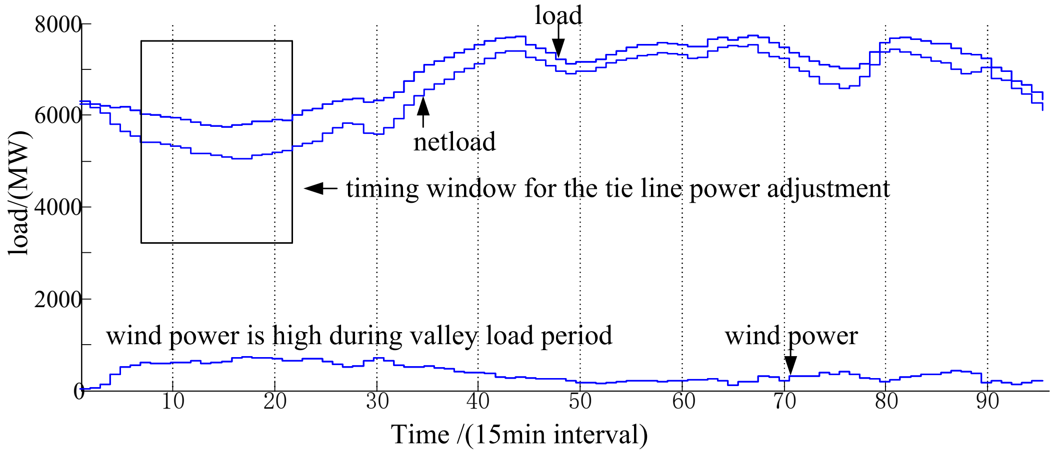

Fig. 1. Typical load and wind power curve of a WCIS in Northern China.

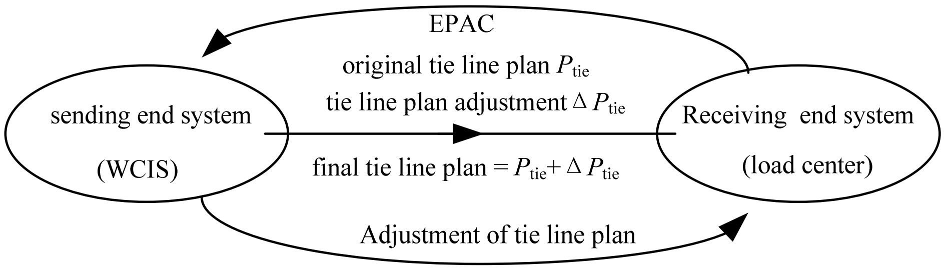

Fig. 2. Simplified topology of IWCIS.

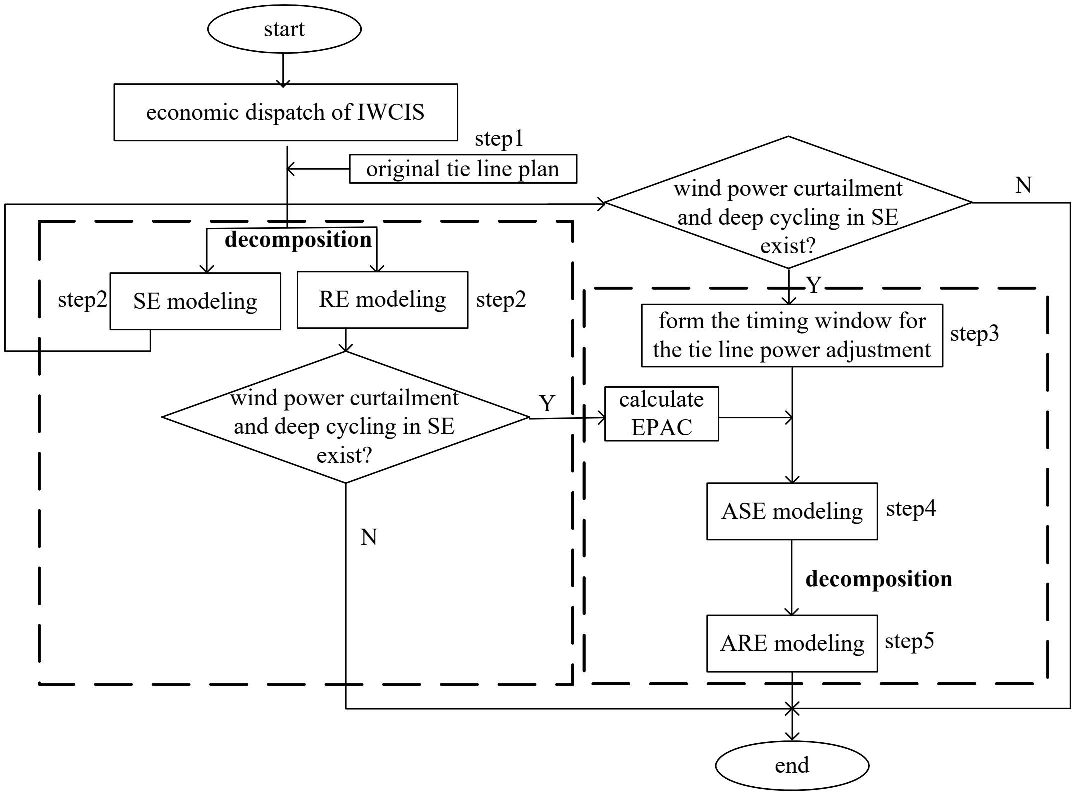

Fig. 3. Flow chart of the adjustment of tie line power plan.

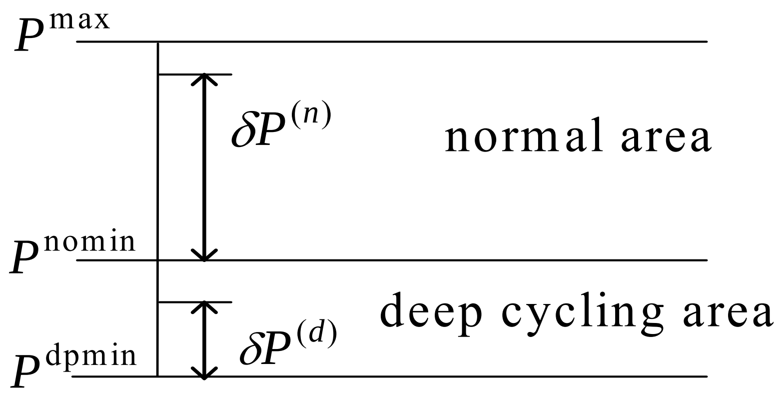

Fig. 4.   Deep cycling model of coal units for generation scheduling.

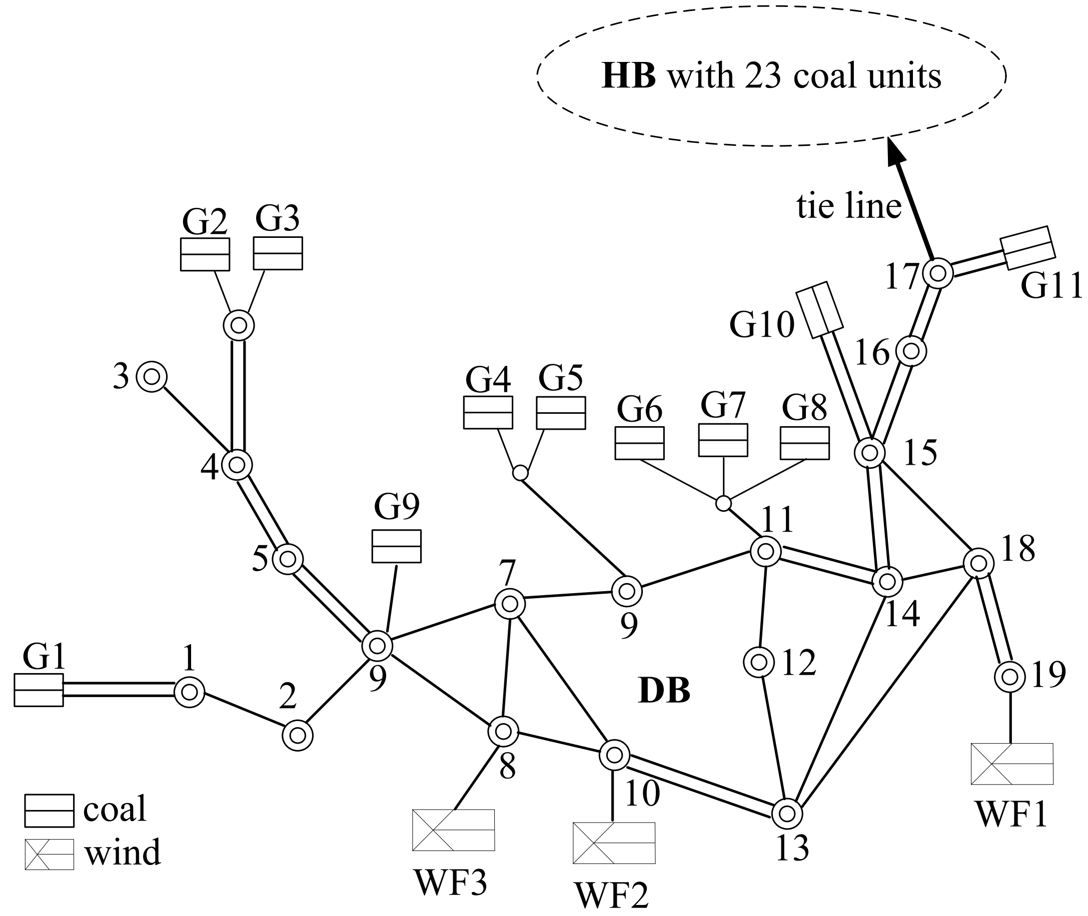

Fig. 5. Geographical diagram of the interconnected DB and HB.

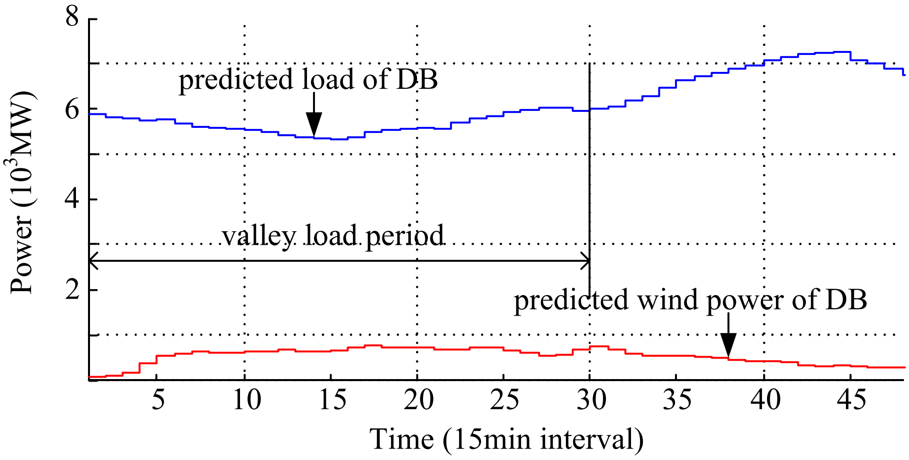

Fig. 6. Predicted load and wind power of DB during valley load period.

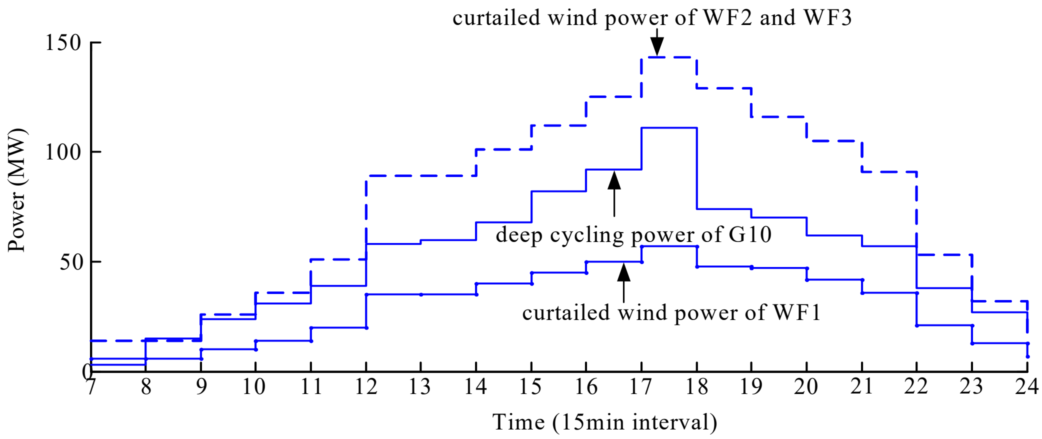

Fig. 7. Deep cycling power and wind power curtailment of system DB during valley load period.

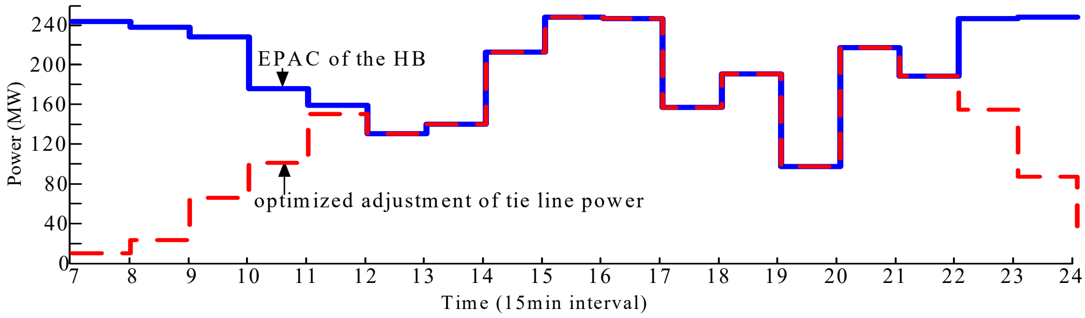

Fig. 8.   Optimal tie line power adjustment.

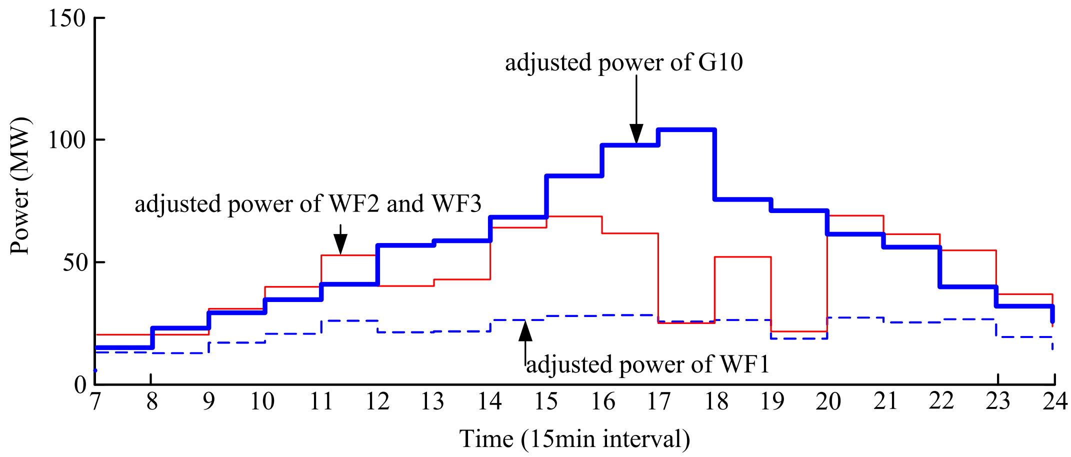

Fig. 9. Power adjustment of deep cycling and wind farm clusters.

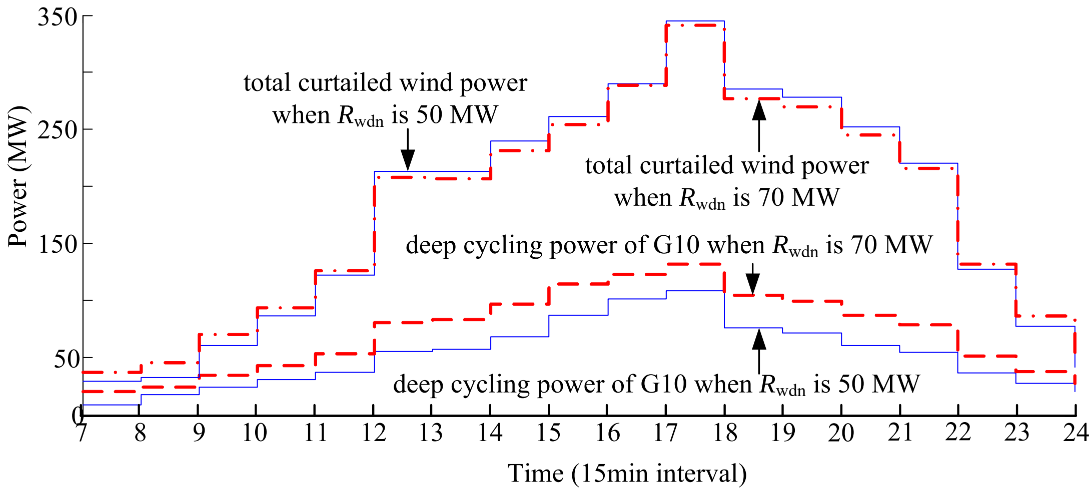

Fig. 10. Deep cycling power of G10 and total curtailed wind power in DB when $R_{wdn,t}$ is 70 MW.

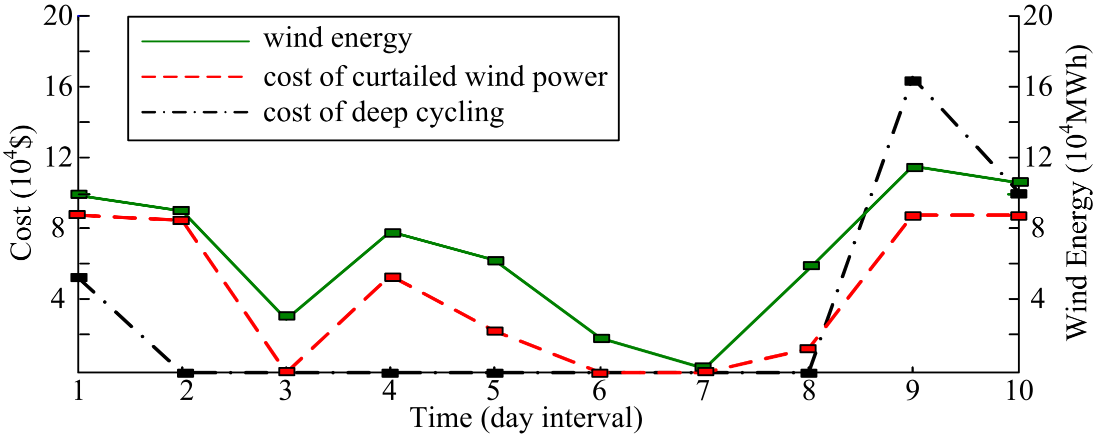

Fig. 11. Daily deep cycling cost and wind power curtailment cost of SC_1.

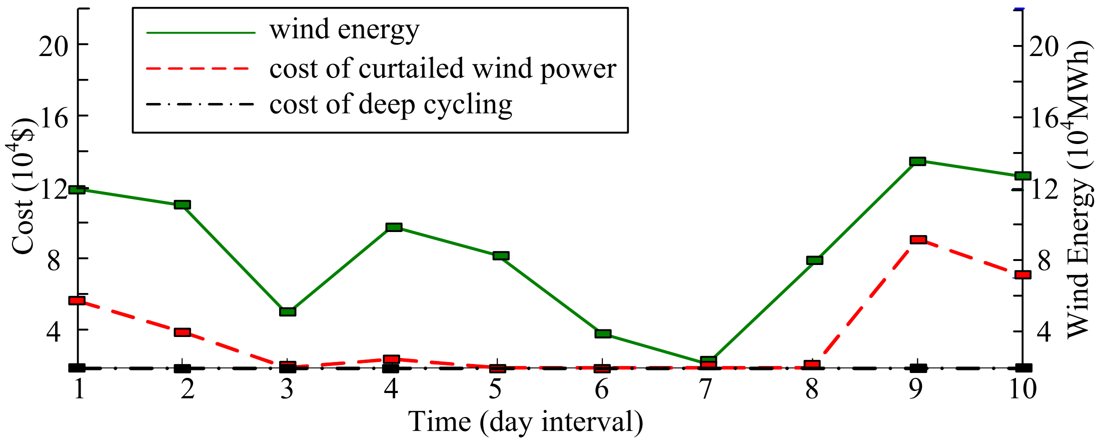

Fig. 12. Daily deep cycling cost and wind power curtailment cost of SC_2.

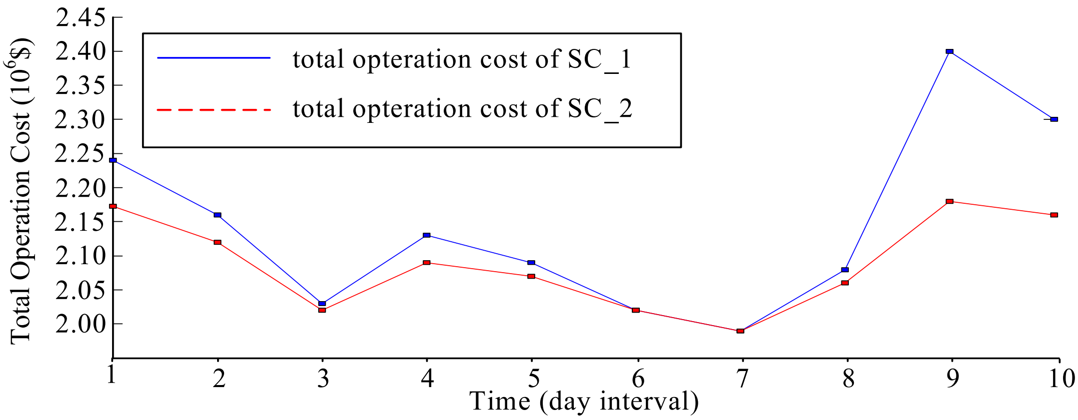

Fig. 13. Total operation cost of SC_1 and SC_2.

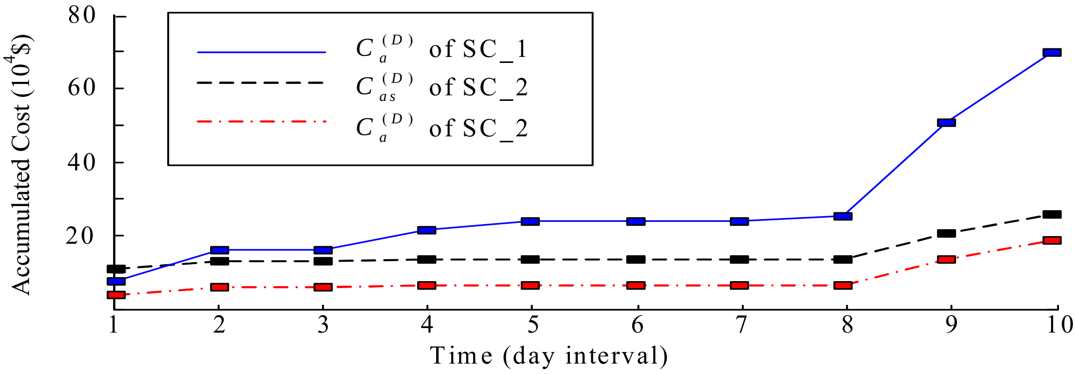

Fig. 14. Accumulated cost of SC_1 and SC_2.

Table 1
Generation equipment of WCIS in Northern China

Power output	Coal	Wind	Nuclear (planned)	Energy storage systems
Max MW	7900	1200	600	200
Min MW	5440	0	600	-150

Table 2

Generating equipment and capacities of DB

	Capacity MW	Percentage of the total capacity %
Total capacity	9100	100.0
Coal power	7900	86.8
Wind power	1200	13.2
Tie line	1500	N/A

Table 3

Original day ahead tie line plan

Time interval	Tie line plan MW	Time interval	Tie line plan MW
1-16	630	49-64	930
17-32	480	65-80	750
33-48	690	81-96	660

Table 4
Parameters of coal units in system DB

		P^{max} MW	P^{nomin} MW	P^{dpmin} MW	$R^{up,max}$ MW	$R^{up,min}$ MW	$R^{dn,max}$ MW	$R^{dn,min}$ MW	r_{up} MW/15min	r_{dn} MW/15min	Start up time h	C_s 10^3\$
Normal unit	G1	1200	900	N/A	100	0	100	0	300	300	26	300
	G2, G3	350	220	N/A	30	0	30	0	75	75	14	130
	G4,G5	550	370	N/A	30	0	30	0	60	60	20	130
	G6-G8	300	200	N/A	30	0	30	0	40	40	18	110
	G9	1600	1000	N/A	220	0	220	0	250	250	24	320
Deep cycling unit	G10	1200	860	600	N/A	N/A	N/A	N/A	150	150	24	350
	G11	1200	900	700	N/A	N/A	N/A	N/A	120	120	24	270
Wind farm	WF1	200	0	N/A	N/A	N/A	N/A	N/A	N/A	N/A	N/A	N/A
	WF2, WF3	500	0	N/A	N/A	N/A	N/A	N/A	N/A	N/A	N/A	N/A

Table 5

Generation scheduling of the system DB during valley load period

Name	Dispatched power output MW											
	5	6	7*	8*	9*	10*	11*	12*	13*	14*	15*	16*
G1	984	975	970	970	970	970	970	970	970	970	970	970
G2, G3	243	230	220	220	220	220	220	220	220	220	220	220
G4, G5	415	406	400	400	400	400	400	400	400	400	400	400
G6-G8	243	236	230	230	230	230	230	230	230	230	230	230
G9	1026	1014	1000	1000	1000	1000	1000	1000	1000	1000	1000	1000
G10 $\delta P^{(d)}$	260	260	252	243	236	230	223	205	203	192	173	159
G10 $\delta P^{(n)}$	24	11	0	0	0	0	0	0	0	0	0	0
G11$\delta P^{(d)}$	200	200	200	200	200	200	200	200	200	200	200	200
G11 $\delta P^{(n)}$	25	11	0	0	0	0	0	0	0	0	0	0
WF1	0	0	5	6	10	14	20	35	35	40	43	48
WF2	0	0	12	13	25	36	51	89	89	100	109	121
WF3	0	0	12	13	25	36	51	89	89	100	109	121
EPAC of HB	246	245	242	237	229	183	168	143	151	215	246	245

Name	Dispatched power output MW											
	17*	18*	19*	20*	21*	22*	23*	24*	25	26	27	28
G1	970	970	970	970	970	970	970	970	975	984	993	991
G2, G3	220	220	220	220	220	220	220	220	231	244	254	252
G4, G5	400	400	400	400	400	400	400	400	407	417	426	424
G6-G8	230	230	230	230	230	230	230	230	236	244	250	249
G9	1000	1000	1000	1000	1000	1000	1000	1000	1015	1027	1040	1037
G10 $\delta P^{(d)}$	152	184	189	200	206	224	233	240	260	260	260	260
G10 $\delta P^{(n)}$	0	0	0	0	0	0	0	0	11	26	39	36
G11 $\delta P^{(d)}$	200	200	200	200	200	200	200	200	200	200	200	200
G11 $\delta P^{(n)}$	0	0	0	0	0	0	0	0	11	26	39	36
WF1	57	47	46	42	36	21	13	7	0	0	0	0
WF2	144	119	116	105	92	53	32	17	0	0	0	0
WF3	144	119	116	105	92	53	32	17	0	0	0	0
EPAC of HB	166	196	114	219	194	245	246	246	166	196	114	219